NUC TP 504

0

ELECTROMAGNETIC FIELDS IN THE OCEAN AND ELECTRORECEPTIVE FISH

by

E. H. Satorius

Undersea Sciences Department

February 1976

NAVAL UNDERSEA CENTER, SAN DIEGO, CA. 92132

AN ACTIVITY OF THE NAVAL MATERIAL COMMAND

R. B. GILCHRIST, CAPT, USN
Commander

HOWARD L. BLOOD, PhD
Technical Director

ADMINISTRATIVE STATEMENT

The work reported herein was conducted during Fiscal Year 1976 at the NUC Marine Life Sciences Laboratory as part of two projects: Electrosensory reception, Project No. SF34371403, sponsored by the Naval Sea Systems Command, and an Independent Research project on Electroreception, S. H. Ridgway, Principal Investigator.

Released by
C. S. Johnson
Associate for Applied Sciences

Under Authority of
B. A. Powell
Head, Undersea Sciences Department

ACKNOWLEDGMENTS

The author wishes to thank R. Seeley, W. Flanigan, S. Ridgway, C. S. Johnson, D. Carder, W. Lowell, W. Kordela, B. Gordon, G. Lindsay, and E. Knudson, for many helpful discussions concerning this report.

UNCLASSIFIED

SECURITY CLASSIFICATION OF THIS PAGE (When Data Entered)

REPORT DOCUMENTATION PAGE — READ INSTRUCTIONS BEFORE COMPLETING FORM

1. REPORT NUMBER: 14 NUC-TP-504	2. GOVT ACCESSION NO.
3. RECIPIENT'S CATALOG NUMBER: 9	
4. TITLE (and Subtitle): 6 ELECTROMAGNETIC FIELDS IN THE OCEAN AND ELECTRORECEPTIVE FISH, (U)	5. TYPE OF REPORT & PERIOD COVERED: Research Report, Jul[redacted]75 - Jul[redacted]76
	6. PERFORMING ORG. REPORT NUMBER
7. AUTHOR(s): 10 E. H. Satorius	8. CONTRACT OR GRANT NUMBER(s): 17 SF34-371-403
9. PERFORMING ORGANIZATION NAME AND ADDRESS	10. PROGRAM ELEMENT, PROJECT, TASK AREA & WORK UNIT NUMBERS: 16 SF34371403
11. CONTROLLING OFFICE NAME AND ADDRESS: Naval Sea Systems Command, Washington, D.C.	12. REPORT DATE: 11 Feb[redacted]77
	13. NUMBER OF PAGES: 35
14. MONITORING AGENCY NAME & ADDRESS (if different from Controlling Office): 12 36p.	15. SECURITY CLASS (of this report): UNCLASSIFIED
	15a. DECLASSIFICATION DOWNGRADING SCHEDULE
16. DISTRIBUTION STATEMENT (of this Report)	
17. DISTRIBUTION STATEMENT (of the abstract entered in Block 20, if different from Report)	
18. SUPPLEMENTARY NOTES	

19. KEY WORDS (Continue on reverse side if necessary and identify by block number)

ocean electromagnetic noise fields
electrosensing skates and sharks

1 microvolt/meter

20. ABSTRACT (Continue on reverse side if necessary and identify by block number)

This report considers the possibility of the detection of dipole fields by electrosensing fish. In particular, a skate (*Raja clavata*) which is sensitive to threshold electric fields of 1 μv/m has been examined. The results indicate that skates detect electric dipole fields at short distances (approximately 100 m at f=0, 1, or 10 Hz and for dipole source current moments on the order of 60 A-m). A comparison between the electric dipole sensing capabilities of skates and artificial systems is also made. In general, it appears that the optimum single-element man-made sensing system is superior to the skate for purposes of long-range detection of

→ narrowband, extremely low-frequency signals.

DD FORM 1473 1 JAN 73 EDITION OF 1 NOV 65 IS OBSOLETE

UNCLASSIFIED

SECURITY CLASSIFICATION OF THIS PAGE (When Data Entered)

390 158

20 (Cont)
narrowband, extremely low-frequency signals.

TABLE OF CONTENTS

1. INTRODUCTION

In this report a study is made of extremely low-frequency ($f \lesssim 10$ Hz) electromagnetic fields in the ocean produced by dipole currents and the possibility of these fields being sensed by electroreceptive fish at various distances from the dipole sources. In Section 2, a brief review of the mechanism for extremely low-frequency passive electroreception by electroreceptive fish is presented. In particular, the electroreception capabilities of a shark, *Scyliorhinus canicula*, and skate, *Raja clavata*, are evaluated. These fish are usually found at the ocean bottom near shore lines and in bays. From an electrical field point of view they are very interesting in that they can sense electric fields as weak as 1 μV/m.* Section 3 of this report deals quantitatively with the electromagnetic fields generated by dipole sources deep in the ocean (i.e., far enough away from ocean-air or earth-ocean boundaries so that boundary effects can be ignored), and the possible detection of these fields by skates. In Section 4, surface electromagnetic waves propagating along the ocean–air interface generated by dipole sources are examined and the possible detection of these surface waves by skates is considered. Finally, in Section 5, a comparison is made of the extremely low-frequency electric-dipole sensing capabilities of skates with the capabilities of man-made extremely low-frequency, electric dipole sensing systems. Sensitivity and environmental noise will be the primary considerations in making this comparison.

The threshold of the skate Raja clavata *has been measured as low as 1 μV/m The threshold of the shark* Scyliorhinus canicula *has been measured at 10 μV/m The threshold value of 1 μV/m for the skate represents the highest electrical sensitivity known in aquatic animals (Ref 1)*

2. A REVIEW OF PASSIVE ELECTRORECEPTION BY ELECTRORECEPTIVE FISH

Certain types of fish have a passive electrosensing mechanism by which they can sense electric fields of very low magnitude. In general, this sensing mechanism is responsive to extremely low-frequency electric fields ($f \lesssim 10$ Hz) at amplitudes (thresholds) which range from 12.5 V/m for *Rhodeus sericeus* down to 1 μV/m for *Raja clavata* (Ref. 1). The electric receptors which make up this electrosensing mechanism in sharks and skates have been identified by Kalmijn (Ref. 4) as the ampullae of Lorenzini.* These ampullae are tiny bladders which are innervated by sensory cells and are connected to surface pores by long canals with highly resistive walls. Each canal is filled with a highly conductive jelly. One side of each of the sensory cells at the bottom of an ampulla is in contact with this jelly, while the other side is in contact with body fluid. When a voltage gradient is applied along the length of one of these electroreceptors, the jelly-side of these sensory cells is at the potential of the jelly nearest the bottom of the ampulla. However, being a good conductor, the jelly nearest the bottom of the ampulla is at the same potential as the seawater at the surface-pore end of the canal (see Fig. 1). The body-fluid side of the sensory cells is at

**Actually, certain fish have passive electrosensing systems which are sensitive to electric fields of much higher frequencies (60-2000 Hz). The electroreceptors which make up this electrosensing system are tuberous sense organs (Ref. 2) This report will concern only the passive electrosensing of extremely low-frequency fields ($f \lesssim 10$ Hz) by ampullary sense organs.*

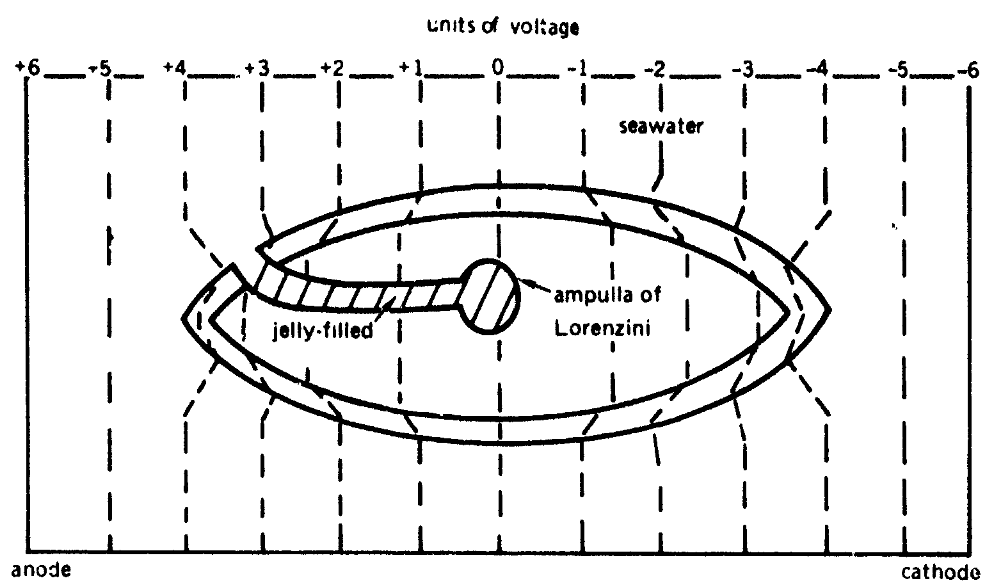

Figure 1 Cross section of electroreceptive fish showing an ampulla of Lorenzini with a voltage gradient applied across its jelly-filled canal. Equipotential lines are shown as dashed lines. Current lines are perpendicular to these equipotential lines Figure adapted from Kalmijn (Ref 1) and Bullock (Ref. 3).

approximately the same potential as that of the seawater at a point just outside the skin nearest the ampulla end of the canal*. Therefore, the ampullary receptor acts like a voltage sensor (see Ref. 1, pp. 189-190), with the long canal enabling the sensory cells to sample the applied voltage gradient at two widely separated points. Sharks and skates have hundreds of these canals, which are oriented in various directions and which reach lengths in skates of up to one-third of the body length (Ref. 3).

The magnitude of the voltage which is sensed by the sensory cells in the ampullae of Lorenzini, when an electric field is applied along the outside of the jelly-filled canal, is given by:**

$$V = \left| \int_C \underline{E}(\underline{r}) \cdot d\underline{s} \right| \tag{1}$$

where V is the magnitude of the sensed voltage; $d\underline{s}$ is a differential distance directed along the canal's longitudinal axis; C represents a path of integration which is parallel to the canal's longitudinal axis, lies completely in the body tissues which surround the canal, and extends from the ampulla to the surface pore; and $\underline{E}(\underline{r})$ is the electric field at the position $\underline{r}$ along the path of integration, C. If the field $\underline{E}(\underline{r})$ is constant along the outside of the canal and parallel to the canal's longitudinal axis, then the integral in Eq. (1) yields:

$$V = |E_0| \ell \tag{2}$$

where $|E_0|$ is the amplitude of the constant electric field and ℓ is the length of the canal. Equation (2) suggests that if the lengths of the largest canals in skates or sharks are proportional to the body lengths of these fish, then the larger sharks and skates should be able to detect lower amplitude threshold electric fields. This is also suggested by Kalmijn (Ref. 4); however, he does not mention whether there was any difference between the longer and shorter skates used in his experiments (these skates (*Raja clavata*) varied from 30 to 60 cm in length) with regards to their responses to the lowest amplitude uniform electric fields applied to these skates. (The applied electric fields in Kalmijn's experiment were 5-Hz square wave fields, amplitude 1 μV/m zero-to-peak.) At present, no experimental evidence can be found which verifies this suggestion.

Although the ampullae of Lorenzini have been identified as the electroreceptors in skates and sharks, it has *not* been shown that structures of this type are responsible for passive electroreception in all electroreceptive fish. As pointed out by Bullock (Ref. 3), ". . . we must not be surprised if some other types [of electroreceptors] turn up in addition."

**The skin of sharks and skates has a low resistance, while the body tissues have a resistance which is much greater than the resistance of seawater. Therefore, voltage gradients in the body tissues are approximately the same as those external to the fish (Ref. 1).*

***This formula is valid for the longer canals when the applied electric fields are large-scale (i.e., generated by large plate electrodes on either side of the fish, or, perhaps, generated by localized sources which are at large distances from the fish as compared to the physical dimensions of the fish). When the applied electric field is a local field (generated by small, closely spaced electrodes placed near the fish), most of the voltage which is sensed by the sensory cells is developed across the skin (Ref. 1). In this report we will mainly be interested in large-scale applied electric fields.*

3. ELECTROMAGNETIC DIPOLE FIELDS IN THE OCEAN (NO BOUNDARY EFFECTS) AND THEIR DETECTION BY SKATES

A. A BRIEF SUMMARY OF ELECTROMAGNETIC WAVE PROPAGATION IN THE OCEAN*

Let us consider electric and magnetic dipole fields. Before writing out the dipole fields (which is done in subsections B and C), a brief summary is given of the equations from which these fields are derived. Electromagnetic propagation in any media can always be characterized by Maxwell's equations,

$$\nabla \times \underline{H} = \underline{J} + j\omega \underline{D} \tag{3}$$

$$\nabla \times \underline{E} = -j\omega \underline{B} \tag{4}$$

$$\nabla \cdot \underline{B} = 0 \tag{5}$$

$$\nabla \cdot \underline{D} = \rho \tag{6}$$

where,

$\underline{E}$ = electric field vector (V/m).

$\underline{H}$ = magnetic field vector (A/m)

$\underline{D}$ = electric displacement vector (coulombs/m^2)

$\underline{B}$ = magnetic induction vector (webers/m^2)

$\underline{J}$ = Source current – density vector (A/m^2)

ρ = Source volume charge density (coulombs/m^3) [See Eq. (7)]

and

ω = angular frequency of the monochromatic fields** (rad/sec)

Combining Eq. (6) with the divergence of Eq. (3) yields the equation of charge continuity:

$$\nabla \cdot \underline{J} = -j\omega\rho \tag{7}$$

The divergence of Eq. (4) yields Eq. (5), and the divergence of Eq. (3) in conjunction with Eq. (7) yields Eq. (6). Therefore, Eqs. (3) through (6) are *not* independent, and constitutive

**For a much more detailed summary, see Kraichman (Ref. 5)*

***One may always obtain the arbitrary time-varying fields from a superposition (Fourier transform) of the monochromatic fields in linear media. For a review of transient fields in conductive media, see Wait (Ref 6).*

relations between the field vectors are needed. For a linear, isotropic medium these constitutive relations may be expressed as follows:

$$\underline{B} = \mu \underline{H} \tag{8}$$

$$\underline{D} = \bar{\epsilon} \underline{E} \tag{9}$$

where μ is the complex magnetic permeability of the medium (in henries/m), and $\bar{\epsilon}$ is the complex electric permittivity of the medium (in farads/m). For the ocean,

$$\mu \gtrsim 4\pi \times 10^{-7} \text{ henries/m} \tag{10}$$

$$\bar{\epsilon} = \epsilon - j\sigma/\omega \tag{11}$$

where

$$\epsilon \approx 80\,\epsilon_0 \text{ and } \epsilon_0 = 8.854 \times 10^{-12} \text{ farads/m}$$

and

$$\sigma \approx 5 \text{ mhos/m (the conductivity of seawater)}$$

Combining Eqs. (3), (4), (8), and (9) yield the wave equation which governs electromagnetic propagation in the ocean:

$$\nabla \times \nabla \times \underline{E} + \gamma^2 \underline{E} = -j\omega\mu \underline{J} \tag{12}$$

where,

$$\gamma^2 = -\omega^2 \mu \bar{\epsilon} = -\omega^2 \mu \epsilon + j\omega\mu\sigma \tag{13}$$

It is Eq. (12) from which the electromagnetic (EM) fields generated by any given source current, J can be derived. In general, the EM field can be expressed as a sum of electric and magnetic multipole fields* (dipole, quadrapole, etc.). In subsections B and C, only the electric and magnetic dipole fields will be of interest, since the mathematical form of these fields is simple and easy to compute plus the fact that dipole fields are good approximations to the EM fields produced by the simplest (and most prevalent) types of antennas (loops and straight wires).** For a good summary of EM fields generated by different types of sources in the ocean, see Refs. 5 and 6.

**See Papas (Ref 7), pp 97-108, or Chapter 16 of Jackson (Ref 8)*

***The equation for electric or magnetic dipole fields [see Eqs (25)-(27) and Eqs (30)-32)] are valid for any straight wire or plane loop (whose length or diameter is smaller than a wavelength) carrying a constant current such that the field observation distance from the wire or loop is much larger (at least 5 times larger) than the length of the wire or the radius of the loop. For observation distances which are close to the current source, the geometry of the source cannot be ignored*

B. ELECTRIC DIPOLE FIELDS IN THE OCEAN

Electric dipole fields are generated by an elementary Hertzian dipole (a very short, straight wire carrying a constant current, I). The electric dipole current which represents a Hertzian dipole may be expressed mathematically as:

$$\underline{J} = \underline{e}_z I \ell \delta(x) \delta(y) \delta(z) \tag{14}$$

where $\underline{e}_z$ is a unit vector pointing in the z-direction; ℓ is the dipole length; and $\delta(x)$ is the Dirac delta function. (For a derivation of Eq. (14), see Ref. 9, pp. 6-8.) Equation (14) corresponds to an electric dipole pointing in the z-direction and located at the center of a Cartesian coordinate system: (x, y, z). Solving Eq. (12) with $\underline{J}$ given by Eq. (14) yields the electric dipole field components (in terms of a spherical coordinate system superimposed over the Cartesian coordinate system, so that $z = r\cos\theta$):

$$E_r = [1/(j\omega\epsilon + \sigma)]\,(I\ell\cos\theta/2\pi r^3)(1 + \gamma r)\,e^{-\gamma r} \tag{15}$$

$$E_\theta = [1/(j\omega\epsilon + \sigma)]\,(I\ell\sin\theta/4\pi r^3)(1 + \gamma r + \gamma^2 r^2)\,e^{-\gamma r} \tag{16}$$

$$H_\phi = (I\ell\sin\theta/4\pi r^2)(1 + \gamma r)\,e^{-\gamma r} \tag{17}$$

It is seen that for DC sources, $\omega = 0$, and the electric dipole field reduces to:

$$E_r = \frac{I\ell\cos\theta}{2\pi\sigma r^3} \tag{18}$$

$$E_\theta = \frac{I\ell\sin\theta}{4\pi\sigma r^3} \tag{19}$$

$$H_\phi = I\ell\sin\theta/4\pi r^2 \tag{20}$$

Notice that H_ϕ is a factor of σ larger, and decreases less with distance than E_r or E_θ for the DC case. For $|\gamma r| \gg 1$, the far-zone EM field is given by (neglecting terms of $1/(\gamma r)^2$ and $1/(\gamma r)^3$):

$$E_r = 0 \tag{21}$$

$$E_\theta = j\omega\mu \frac{I\ell\sin\theta}{4\pi r} e^{-\gamma r} \tag{22}$$

$$H_\phi = \frac{I\ell\gamma\sin\theta}{4\pi r} e^{-\gamma r} \tag{23}$$

Notice that in the far field:

$$|E_\theta/H_\phi| = \left|(1 + j)\sqrt{\frac{\omega\mu}{2\sigma}}\right| \qquad (\text{for } \sigma \gg \omega\epsilon) \tag{24}$$

The quantity

$$Z_0 = (1+j)\sqrt{\frac{\omega\mu}{2\sigma}}$$

represents the characteristic impedance of the ocean to EM wave propagation. In the ocean, for $\sigma \gg \omega\epsilon$, note that Eqs. (15)-(17) can be written:

$$E_r = \frac{I\,\ell \cos\theta}{2\pi\sigma r^3}(1+\gamma r)\,e^{-\gamma r} \tag{25}$$

$$E_\theta = \frac{I\,\ell \sin\theta}{4\pi\sigma r^3}(1+\gamma r+\gamma^2 r^2)\,e^{-\gamma r} \tag{26}$$

$$H_\phi = \frac{I\,\ell \sin\theta}{4\pi r^2}(1+\gamma r)\,e^{-\gamma r} \tag{27}$$

Where $\gamma \approx \sqrt{j\sigma\mu\omega} = (1+j)\sqrt{\sigma\mu\omega/2}$.* In Figs. 2 and 3, the functions $|(1+\gamma r)\,e^{-\gamma r}| = B$ and $|(1+\gamma r+\gamma^2 r^2)\,e^{-\gamma r}| = A$ are plotted.

Throughout the rest of this report, it is assumed that $\gamma = (1+j)\sqrt{\sigma\mu\omega/2}$, viz., $\sigma \gg \omega\epsilon$. This is a good assumption in sea-water for frequencies less than 10^9 Hz (Ref 10)

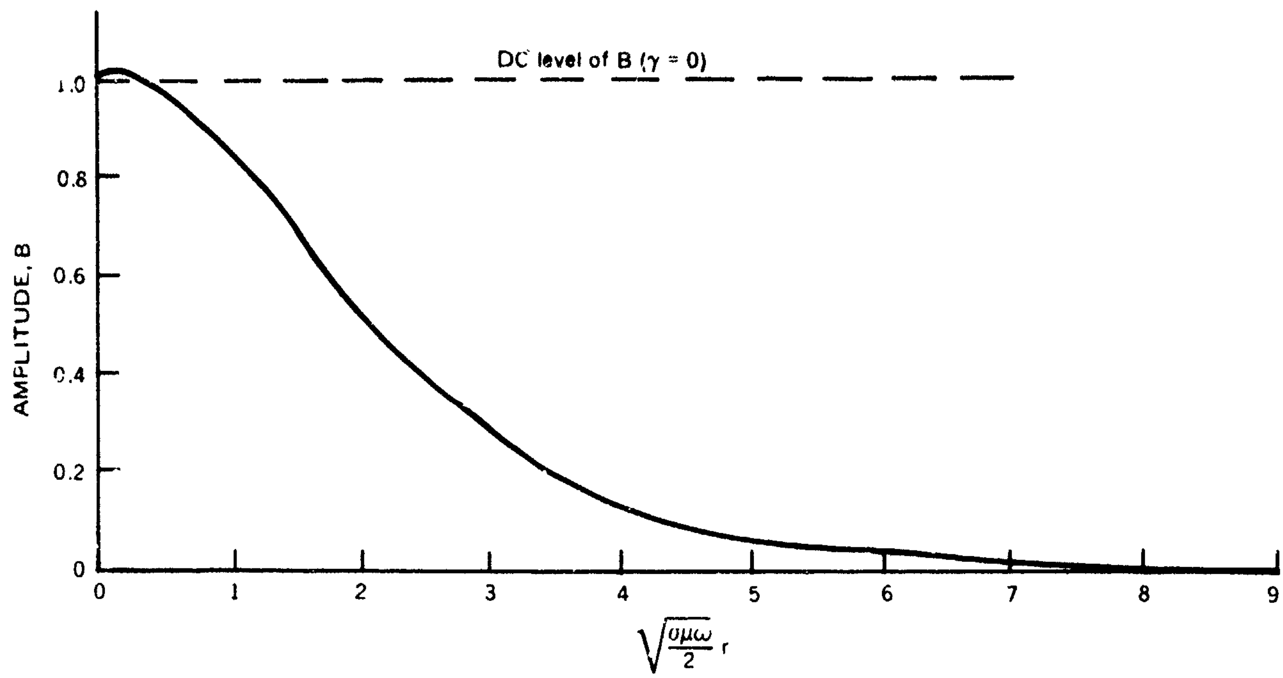

Figure 2. The function $B = |(1+\gamma r)\,e^{-\gamma r}|$ vs $\sqrt{\frac{\sigma\mu\omega}{2}}\,r$.

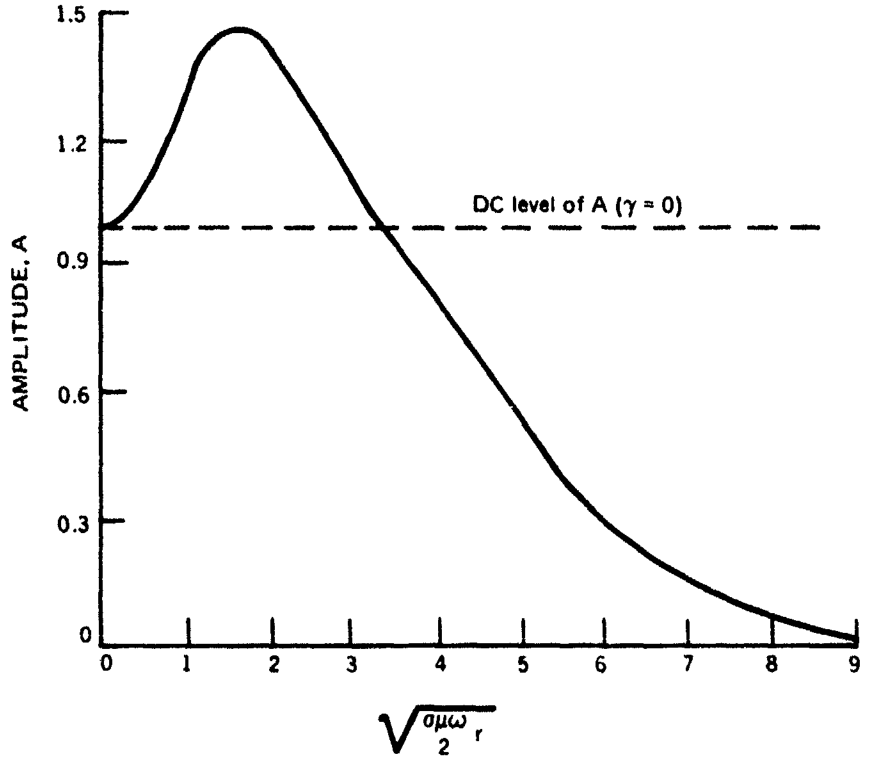

Figure 3. The function $A = |(1 + \gamma r + \gamma^2 r^2)\, e^{-\gamma r}|$ versus $\sqrt{\frac{\sigma\mu\omega}{2}}\, r$.

In examining the possible detection of electric dipole fields by skates (threshold = 1 μV/m), we are interested in the magnitudes $|E_r|$ and $|E_\theta|$. In Fig. 4, $|E_r|$, $|E_\theta|$, and $|H_\phi|$ are plotted for f = 1 Hz.

In Fig. 5, $|E_r|$, $|E_\theta|$, and $|H_\phi|$ are plotted for f = 10 Hz. In Fig. 6, $|E_r|$, $|E_\theta|$, and $|H_\phi|$ are plotted for DC fields.

In Figs. 4, 5, and 6, $I\ell = 4\pi\sigma \approx$ 60 A-m. This particular value for the current moment, $I\ell$, was chosen so that at 1 m

$$|E_\theta|_{\theta = \pi/2} = 1 \text{ V/m}$$

at DC (in seawater). It is seen in Figs. 4, 5, and 6, that for this particular value of $I\ell$, both

$$|E_\theta|_{\theta = \frac{\pi}{2}}$$

and

$$|E_r|_{\theta = 0}$$

reach the threshold level of skates in a very short distance (approximately 100 m for all three cases - f = 0, 1, 10 Hz). It would require a tremendous current moment, $I\ell$, to make

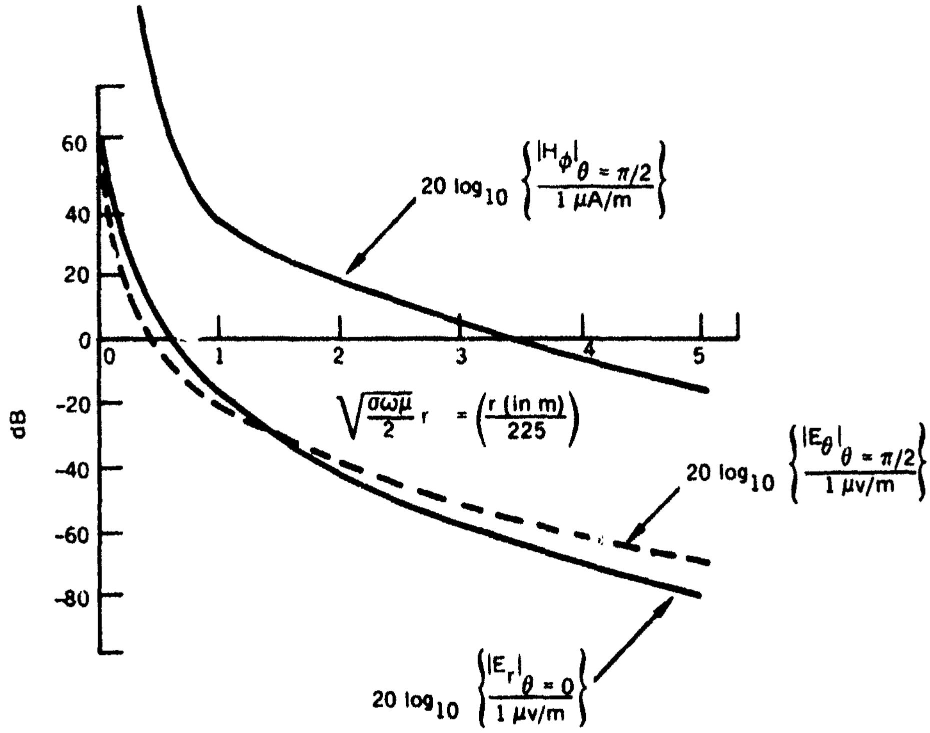

Figure 4. $|E_r|_{\theta=0}$, $|E_\theta|_{\theta=\frac{\pi}{2}}$, and $|H_\phi|_{\theta=\pi/2}$ in decibels (relative to 1 μV/m or 1 μA/m) vs $\sqrt{\frac{\sigma\mu\omega}{2}}\, r$ (= r(in m)/225) for $I\ell = 4\pi a \approx 60$ A-m and f = 1 Hz.

the electric fields extend very far in the ocean. For instance, suppose the electric field

$$|E_\theta|_{\theta=\pi/2}$$

were to reach a value of 1 μV/m at 1000 km for f = 0. This implies [from Eq. (26)] that $10^{-6} = I\ell/(20 \times 10^{18})$, or, $I\ell \approx 6.3 \times 10^{13}$ A-m. This would require a current of 6.3×10^{13} A in a wire 1 m long, or, equivalently, a current of 1 A in a wire 6.3×10^{13} m long! For the DC electric field to reach a value of 1 μV/m at 1 km would still require a current moment of approximately 6×10^4 A-m. At either f = 1 Hz or f = 10 Hz, the required current moments for the electric dipole fields to reach a value of 1 μV/m at 1000 km and 1 km would be orders of magnitude greater than 6.3×10^{13} A-m and 6×10^4 A-m respectively, due to the presence of the exponential attenuation factor $e^{-\gamma r}$ in Eqs. (25)-(27). It is

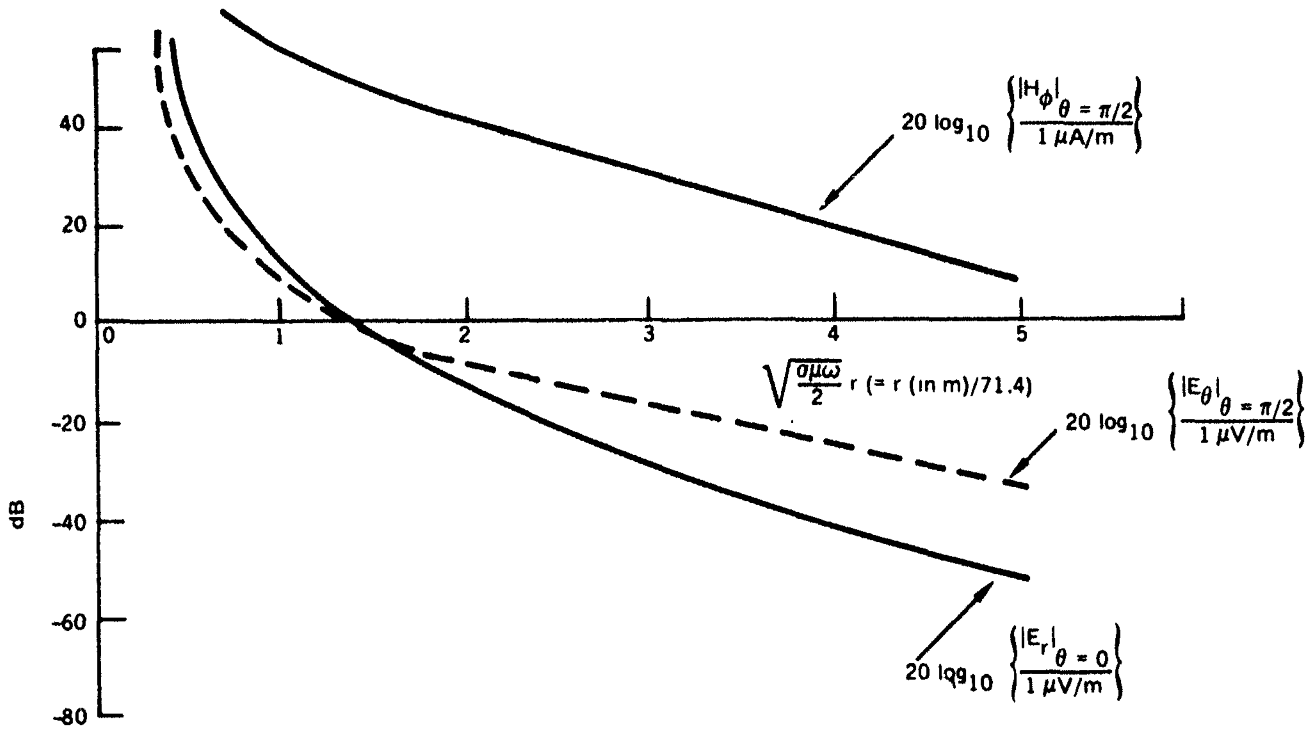

Figure 5. $|E_r|_{\theta=0}$, $|E_\theta|_{\theta=\pi/2}$, and $|H_\phi|_{\theta=\pi/2}$ in decibels (relative to 1 μV/m or 1 μA/m) versus $\sqrt{\frac{\sigma\mu\omega}{2}}$ r (= r(in m)/71.4) for $I\ell = 4\pi\sigma \approx$ 60 A-m and f = 10 Hz.

noted that for a *hypothetical* "magnetic" fish sensitive to magnetic fields* of 1 μA/m (0.001 gamma), it would be possible to sense the electric dipole field further away than for an electric field-sensing fish. For instance, at f = 0 Hz (Fig. 6), a "magnetic" fish could sense an electric dipole field (for $I\ell \approx$ 60 A-m) at 1 km. For f = 1 Hz (Fig. 4), this threshold distance is approximately 900 m and for f = 10 Hz (Fig. 5), the threshold distance is approximately 380 m. Therefore, the sensing of electric dipole fields at extremely low frequencies (f $\lesssim$ 10 Hz) by the most sensitive electroreceptive fish known (*Raja clavata*) is limited to relatively short distances (approximately 100 m for current moments on the order of 60 A-m).

**As pointed out by Kalmijn (Ref 1), electroreceptive fish could sense a magnetic field, $\underline{B}$, by moving through the field at a velocity, $\underline{v}$, which is perpendicular to $\underline{B}$. This motion produces a potential gradient of magnitude $|\underline{v}|\,|\underline{B}|$, which the fish senses. However, the threshold level of the magnetic field which the most sensitive fish (threshold ≈ 1 μV/m) could measure would be given by $\underline{B}$ = 1 emu/(100 cm/sec) = 0.01 gauss (assuming the fish could reach a velocity of 100 cm/sec). This value for the threshold level of the magnetic field is quite high (i e , 0.01 gauss is approximately 2 5% of the earth's magnetic field), and an electroreceptive fish would be better off (in terms of detection distance) to directly sense the electric part of the above-mentioned electromagnetic fields*

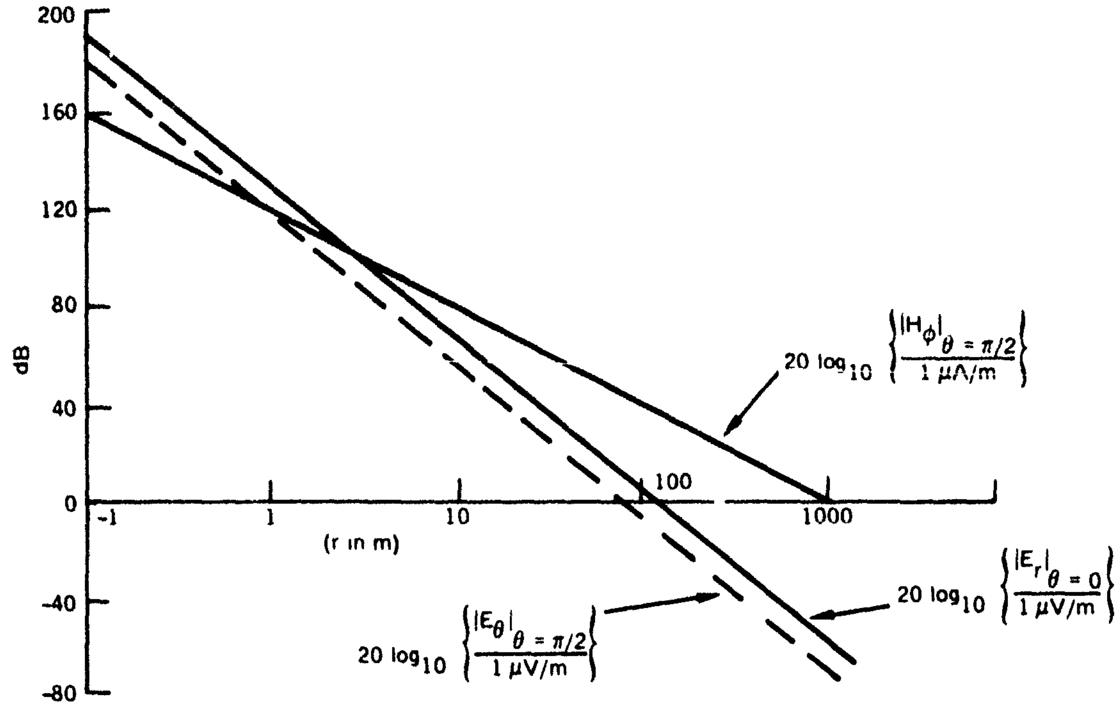

Figure 6. $|E_r|_{\theta=0}$, $|E_\theta|_{\theta=\pi/2}$, and $|H_\phi|_{\theta=\pi/2}$ in decibels (relative to 1 μV/m or 1 μA/m) vs r (in m) for $I\ell \approx 4\pi\sigma \approx 60$ A-m and f = 0 Hz

C. MAGNETIC DIPOLE FIELDS IN THE OCEAN

Magnetic dipole fields are generated by elementary loop currents (a very small plane loop carrying a constant current I). The generating electric current of a magnetic dipole field is given by (Ref. 9):

$$\underline{J} = \nabla \times \underline{M}^0 \tag{28}$$

where,

$$\underline{M}^0 = \underline{e}_z\, I\, \Delta a\, \delta(x)\, \delta(y)\, \delta(z) \tag{29}$$

In Eq. (29), Δa is the area of the plane loop, and all other symbols are as defined in Eq. (14). The positive normal to the plane loop current [defined by Eqs. (28) and (29)] is parallel to the z-axis. Solving Eq. (12) with $\underline{J}$ given by Eq. (28) yields the magnetic dipole field components (in terms of the same coordinate system used in subsection B):

$$E_\phi = \frac{-j\mu\omega\, I\, \Delta a}{4\pi r^2}\,(1 + \gamma r)\, e^{-\gamma r} \sin\theta \tag{30}$$

$$H_r = \frac{I\,\Delta a}{2\pi\,r^3}(1+\gamma r)\,e^{-\gamma r}\cos\theta \tag{31}$$

$$H_\theta = \frac{I\,\Delta a}{4\pi\,r^3}(1+\gamma r+\gamma^2 r^2)\,e^{-\gamma r}\sin\theta \tag{32}$$

For DC currents, $\gamma = 0$, and the magnetic dipole reduces to:

$$E_\phi = 0 \tag{33}$$

$$H_r = \frac{I\,\Delta a\cos\theta}{2\pi\,r^3} \tag{34}$$

$$H_\theta = \frac{I\,\Delta a\sin\theta}{4\pi\,r^3} \tag{35}$$

It is noted that the electric field vanishes for $f = 0$. For $|\gamma r| \gg 1$, the far-zone EM field is given by:

$$E_\phi = \frac{-j\mu\omega\,\gamma\,I\,\Delta a}{4\pi\,r}\sin\theta\;e^{-\gamma r} \tag{36}$$

$$H_r = 0 \tag{37}$$

$$H_\theta = \frac{I\,\Delta a\,\gamma^2}{4\pi\,r}\sin\theta\;e^{-\gamma r} \tag{38}$$

It is seen from Eqs. (31) and (32) that H_r and H_θ for the magnetic dipole field is equivalent to E_r and E_θ for the electric dipole field (with $I\,\Delta a$ replaced by $I\ell/\sigma$). In Fig. 7, $|E_\phi|$, $|H_r|$, and $|H_\theta|$ are plotted for f = 1 Hz. In Fig. 8, $|E_\phi|$, $|H_r|$, and $|H_\theta|$ are plotted for f = 10 Hz. In Fig. 9, $|H_r|$ and $|H_\theta|$ are plotted for DC fields (f = 0 Hz).

Note that in Figs. 7, 8, and 9, $I\,\Delta a = 4\pi$ A-m^2 $\approx$ 12 A-m^2 so that at r = 1 m (for DC)

$$|H_\theta|_{\theta=\pi/2} = 1\ \mathrm{A\ m^{-1}}\,.$$

It is seen from these figures that for this particular value of $I\,\Delta a$, $|E_\phi|$ reaches the threshold of skates in an incredibly short distance (approximately 2 m for f = 1 Hz and 7 m for f = 10 Hz).* It is also seen that the magnetic fields (for $I\,\Delta a \approx$ 12 A-m^2) of magnetic dipoles fall off in exactly the same way as do the electric fields of an electric dipole field (Figs. 4, 5, and 6) as noted above. Therefore, a hypothetical "magnetic" fish which is sensitive to a magnetic field of 1 μA/m (0.001 gamma) could detect magnetic dipole fields (f = 0, 1, 10 Hz and $I\,\Delta a \approx$ 12 A-m^2) out to approximately 100 m.

*At DC, electric fish can still detect magnetic dipole fields by moving perpendicular to the DC magnetic field (as discussed previously). However, if the fish is sensitive to 1 μV/m and can move at a velocity of 1 m/sec, it will only be able to detect the dc magnetic dipole field ($I\,\Delta a \approx$ 12 A-m^2) out to approximately 1 m.

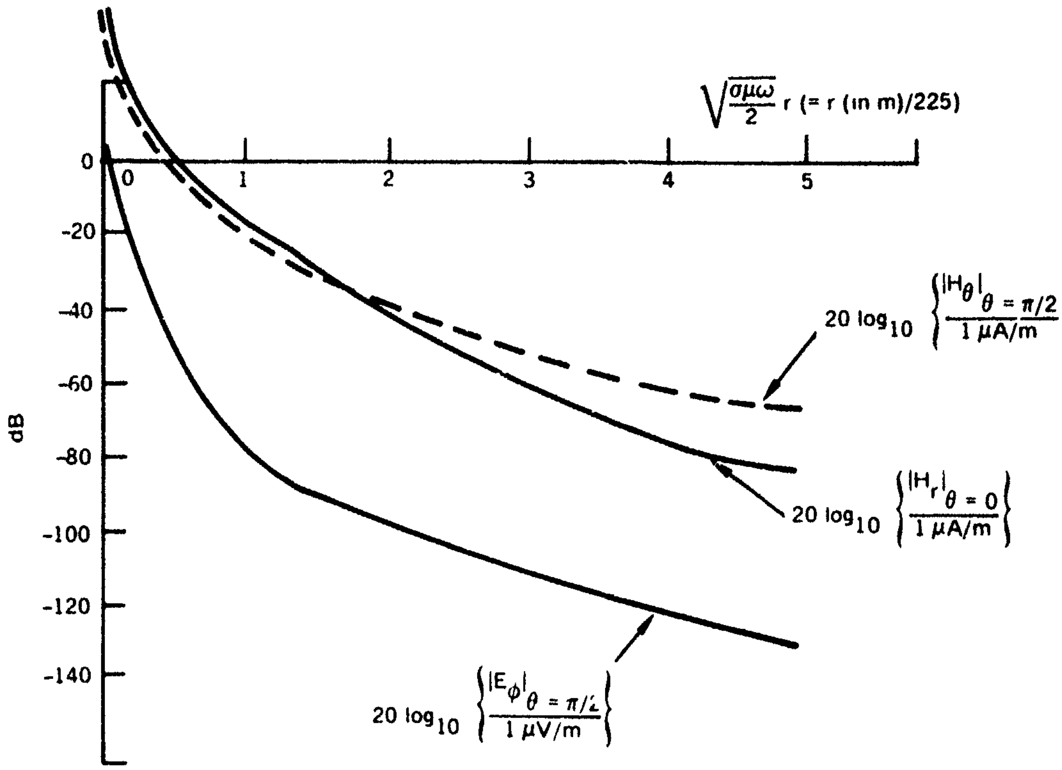

Figure 7. $|H_r|_{\theta = 0}$, $|H_\theta|_{\theta = \pi/2}$, and $|E_\phi|_{\theta = \pi/2}$ in decibels (relative to 1 μA/m or 1 μV/m) vs. $\sqrt{\frac{\sigma\omega\mu}{2}}\, r$ (= r(in m)/225) for $I\,\Delta a = 4\pi$ A-m^2 and f = 1 Hz.

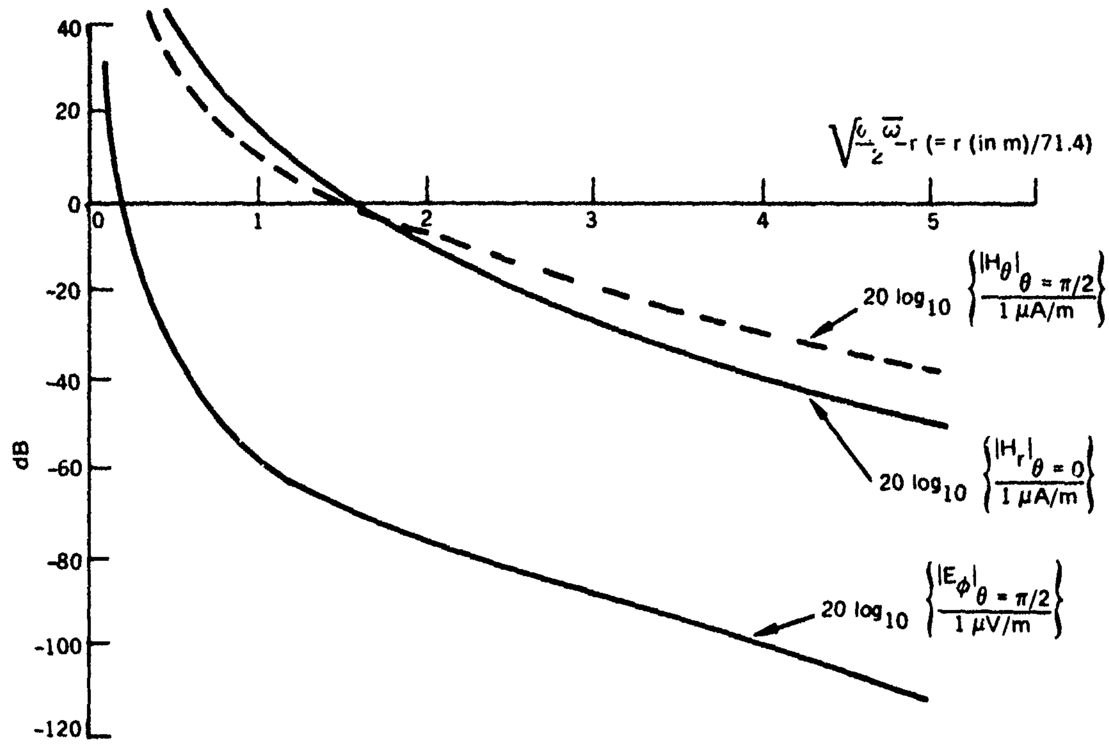

Figure 8. $|H_r|_{\theta=0}$, $|H_\theta|_{\theta=\pi/2}$, and $|E_\phi|_{\theta=\pi/2}$ in decibels (relative to 1 μA/m or 1 μV/m) versus $\sqrt{\frac{\sigma\mu\omega}{2}}\,r$ (= r (in meters)/71.4) for $I\,\Delta a = 4\pi$ A-m^2 and f = 10 Hz.

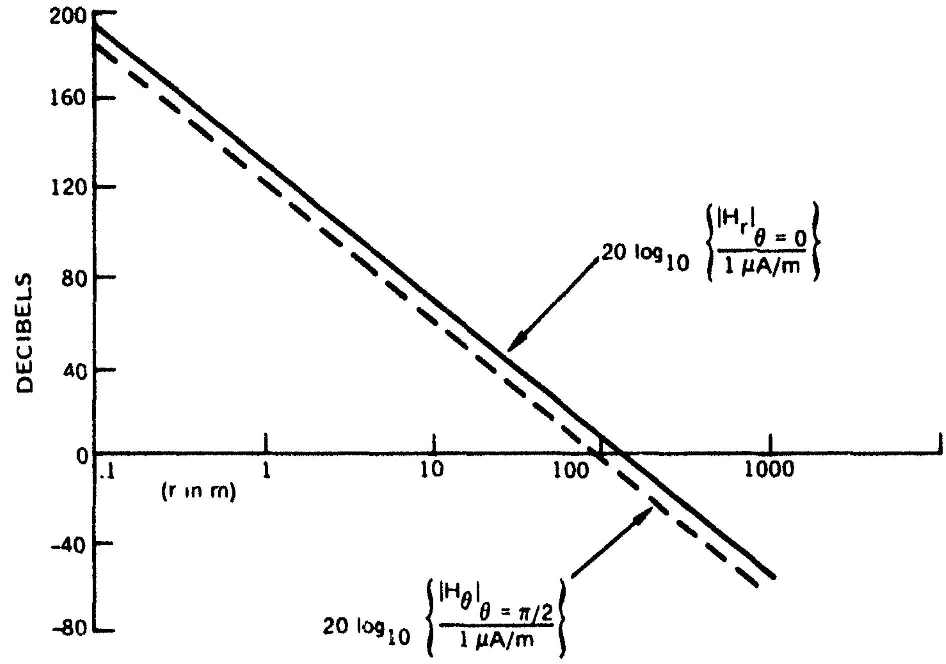

Figure 9. $|H_r|_{\theta=0}$ and $|H_\theta|_{\theta=\pi/2}$ in decibels (relative to 1 μA/m) versus r (in meters) for I Δa = 4π A-m^2 and f = 0 Hz

4. ELECTROMAGNETIC WAVES TRAVELING ALONG THE OCEAN'S SURFACE AND THE POSSIBILITY OF THEIR DETECTION BY SKATES

Asiue from the possibility of detecting electrical dipole fields which propagate directly through the ocean, electroreceptive fish could, in principle, detect electrical dipole fields which are generated in the ocean and travel up to and along the ocean's surface and then leak back down to the electric fish.* This up-over-and-down mode of propagation which has been analyzed in detail with regard to submarine communication** is depicted graphically in Fig. 10.

In this section this up-over-and-down mode of propagation of electrical signals will be considered. It is possible that skates could detect electrical signals following such an indirect path since, as will be seen, signals following this path are exponentially attenuated much less than signals following the direct path (through the ocean) from source to skate.

**Presumably, electroreceptive fish could also detect electric fields which travel along the ocean bottom. However, for brevity, these fields will not be considered (For a study of electrical fields propagating along the ocean bottom, see Ref. 11.)*

***For a good review of submarine communication and the up-over-and-down mode of electromagnetic propagation, see Ref. 12.*

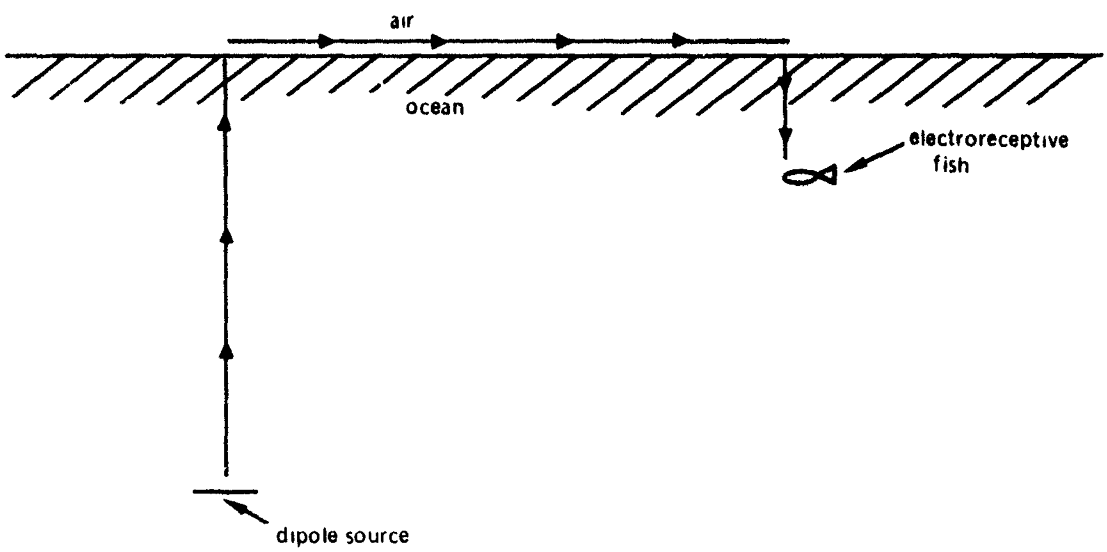

Figure 10. Up-over-and-down path of electric field propagation in the ocean. (Arrows indicate path of electric signal.)

As a matter of fact, the exponential attenuation of electrical signals following the up-over-and-down path is given by $e^{-D/\delta}$ [see Eqs. (40)–(42)], where $\delta = \sqrt{2/\mu\omega\sigma}$ is the skin depth. (which is the depth in the ocean at which electromagnetic fields are reduced by approximately 9 dB from their value at the surface) and D is the combined vertical depth of the dipole source and the skate. For f = 1 Hz and 10 Hz, exponential attenuation of approximately 9 decibels will occur at D ≈ 225 m and D ≈ 70 m, respectively. Therefore, for skates near the surface (less than 50 ft), the dipole source at 1 Hz may be submerged to a depth of 700 ft (or 200 ft at 10 Hz) and only 9 dB exponential attenuation will result. [Of course, inverse R^2 and R^3 losses (where R is the distance from the dipole source to the ray) will still be present. See Eqs. (40)–(42).] It is for this reason that the up-over-and-down path of propagation is considered as a possible means of detection of dipole fields by electroreceptive fish. (For brevity and because a horizontal (parallel to the water's surface), electric dipole produces the strongest electromagnetic surface wave (see Ref. 9, pp. 232–235) only a horizontal electric dipole as the source of the electromagnetic field for the up-over-and-down path of propagation will be considered.)

Baños (Ref. 9), in an excellent treatise on dipole radiation in the presence of a conducting half-space, has derived extremely useful approximations for the electromagnetic fields generated by electric and magnetic dipoles submerged in a conductive half-space.* The coordinate system used by Baños is a cylindrical coordinate system centered on the ocean's surface directly above the electric dipole (see Fig. 11). The horizontal, electric dipole current source is represented by:

$$\underline{J} = \underline{e}_x I\ell\, \delta(x)\, \delta(y)\, \delta(z+h) \tag{39}$$

where $\underline{e}_x$ is the unit vector pointing in the x-direction, h is the depth of the dipole, and all other symbols are as defined in Eq. (14). The expressions for the electric field components in the ocean are given by (see Ref. 9, p. 209):

$$E_{1r} = \frac{I\ell \cos\phi}{2\pi\sigma r^3} e^{-\gamma(h-z)} \tag{40}$$

$$E_{1\phi} = \frac{I\ell \sin\phi}{\pi\sigma r^3} e^{-\gamma(h-z)} \tag{41}$$

$$E_{1z} = j\frac{\gamma I\ell \cos\phi}{2\pi\sigma r^2} \frac{\omega\epsilon_0}{\sigma} e^{-\gamma(h-z)} \tag{42}$$

For purposes of reference, the expression for the dominant z-component of the electrical field in the air just above the ocean's surface will also be given:

$$E_{2z} = \frac{\gamma I\ell \cos\phi}{2\pi\sigma r^2} e^{-\gamma h} \tag{43}$$

As in Section 3, γ in the above formulas is given (to a very good approximation) by $(1 + j)\cdot\sqrt{\sigma\mu\omega/2}$.

Sommerfeld (Ref 13) was the first to consider dipole radiation near a conductive half-space.

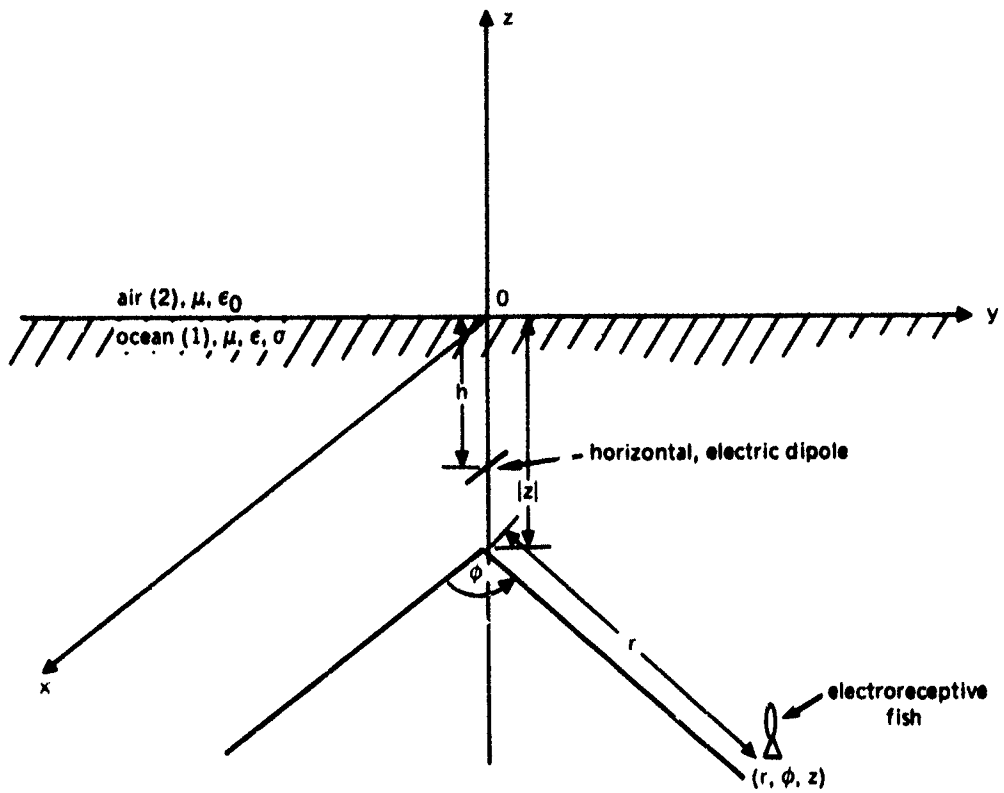

Figure 11. Coordinate system showing the position of the source and the electroreceptive fish. Note that at the position of the electroreceptive fish, $z < 0$.

It is *very important* to note the region of validity in which Eqs. (40)–(43) hold. First of all, the dipole source as well as the electroreceptive fish (skate) must be close to the ocean–air interface, viz., the condition $h,z \ll r$, where r is the horizontal distance from the source to the skate (see Fig. 11), must be satisfied. The condition $\omega/c\, r < 1 < |\gamma r|$ should also be satisfied. This latter condition implies that the horizontal distance between source and skate exceeds several wavelengths in the conducting medium, but amounts to only a small fraction of a free-space wavelength. Since free-space wavelengths at frequencies which are of interest here ($f \lesssim 10$ Hz) are quite long ($c/\omega \gtrsim 5 \times 10^6$ m) and the ocean wavelengths in this frequency range are quite short in comparison ($1/|\gamma| \lesssim 300$ m), it is this region of validity (which Baños calls the "near-field region") which is of interest in this report. Actually, the quasistatic region ($0 \lesssim \omega/c\, r < 1$) is also important for our considerations; however, formulas valid in this region are quite similar (see Ref. 9, Chapter 4). In any case, the near-field formulas are quite useful in establishing an upper bound on the detection distance for detecting submerged sources (via the up-over-and-down path) by electroreceptive fish (or any electrical sensor). Note that aside from the contributions to the electrical field given by Eqs. (40)–(43), there are also contributions due to the effects of the ionosphere (see Ref. 14). However, in the ranges of horizontal distance from source to skate which are important here, these ionospheric effects can be neglected.

In Fig. 12,

$$|E_{1r}|_{\phi=0},\ |E_{1\phi}|_{\phi=\pi/2},\ \text{and}\ |E_{2z}|_{\phi=0}$$

are plotted for f = 1 Hz and 10 Hz and $I\ell = 4\pi\sigma \approx 60$ A-m. Plots of

$$|E_{1z}|_{\phi=0}$$

will not be included since this component of the electric field is negligible

$$\left(20 \log_{10}\left\{\frac{|E_{1z}|_{\phi=0}}{1\,\mu V/m}\right\} < -120 \text{ dB for both f = 1 Hz and 10 Hz and } r \geqslant 1 \text{ m}\right).$$

Also, since Eqs. (40)–(43) are only valid for $r > 1/|\gamma|$, all plots will start at $r \approx 1/|\gamma|$. In Fig. 12, no exponential attenuation losses have been included, although these losses are easily included by subtracting 9 dB per skin depth submersion from the levels shown for

$$|E_{2z}|_{\phi=0},\ |E_{1r}|_{\phi=0},\ \text{and}\ |E_{1\phi}|_{\phi=\pi/2}.$$

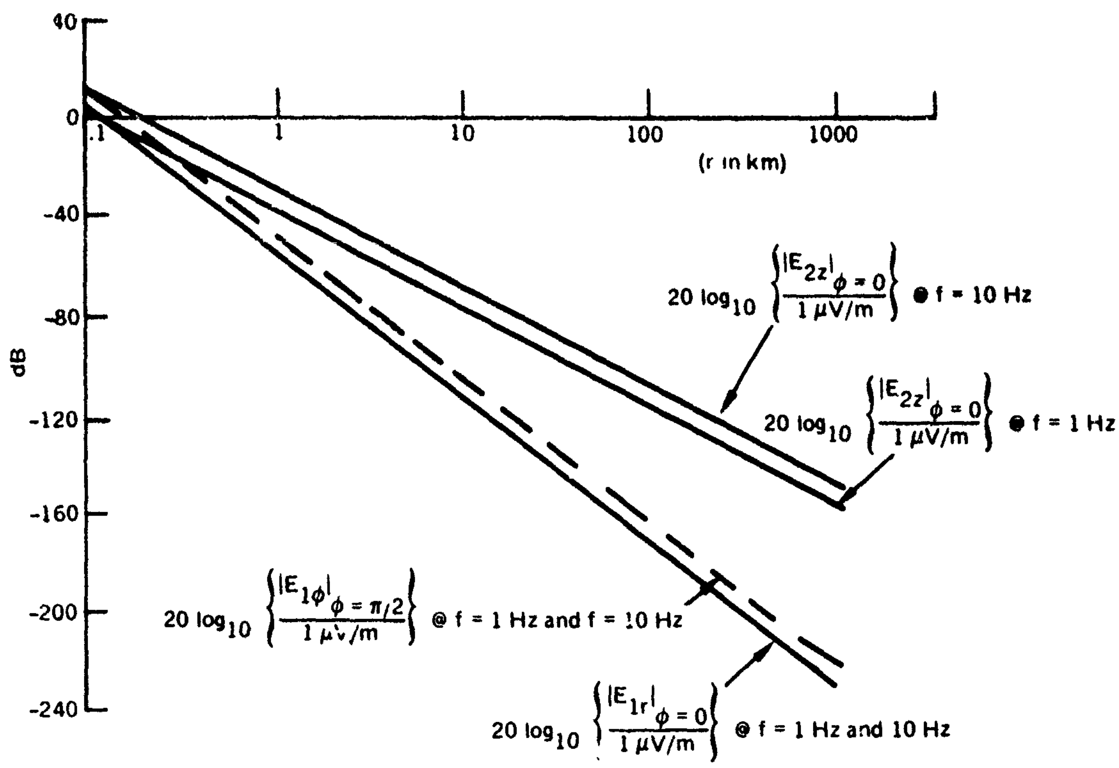

Figure 12 $|E_{1r}|_{\phi=0}$, $|E_{1\phi}|_{\phi=\pi/2}$, and $|E_{2z}|_{\phi=0}$ in decibels (relative to 1 μV/m) versus r (in kilometers) for $I\ell = 4\pi\sigma \approx 60$ A-m at f = 1 Hz and f = 10 Hz.

As can be seen from Fig. 12, for $I\ell \approx 60$ A-m, the range of detection of a horizontal electric dipole by the most sensitive skate (via the up-over-and-down path) is limited to approximately 100 m, which is about the same range as for the direct path (see Figs. 4, 5, and 6). Actually, 100 m is slightly outside the region of validity of the formulas [Eqs. (40)–(43)] for f = 1 Hz, however, by using the formulas appropriate for the 100-m range (quasistatic formulas) one would still arrive at a value of approximately 100 m as the upper bound for detection by skates of electric dipoles via the up-over-and-down path at f = 1 Hz. For the fields to extend much further than 100 m, incredible current moments are needed. For instance, a current moment of approximately 6×10^{13} A-m is needed for the dipole fields to be detected at 1000 km at either 1 Hz or 10 Hz. For detection at 1 km, a current moment of approximately 6×10^4 A-m would be required at either 1 Hz or 10 Hz. (Note that $|E_{2z}|$, the normal electric field component in air, falls off less rapidly than either $|E_{1\phi}|$ or $|E_{1r}|$. However, this component, $|E_{2z}|$, is down to 1 μV/m at a horizontal distance of approximately 300 m for $I\ell \approx 60$ A-m and f = 1 Hz or 10 Hz.) Therefore, the sensing of horizontal electric dipole fields via the up-over-and-down path of propagation at extremely low frequencies ($f \lesssim 10$ Hz) by the most sensitive electroreceptive fish (*Raja clavata*) is limited to short distances (approximately 100 m for current moments on the order of 60 A-m).

5. A COMPARISON BETWEEN THE ELECTRIC-SENSING CAPABILITIES OF SKATES AND ARTIFICIAL SYSTEMS

In this section a comparison is given of the electric dipole sensing capabilities of a skate (*Raja clavata*) with those of man-made systems with regard to the maximum detection distance (MDD) of a narrowband, extremely low-frequency ($f \lesssim 10$ Hz), electrical signal generated by an electrical dipole.* In particular, two different types of artificial systems will be examined. The first, which is an underwater system, will consist of one electric field sensing antenna (a pair of highly conductive plates, a receiving toroid, etc.) which is connected to a sensor (bandpass filter and voltage sensor). The second type of sensing system considered consists of one sensing antenna which is placed above the ocean's surface.** This antenna is also assumed to be connected to a sensor.† The performance of these different types of artificial systems will be compared with the electric dipole sensing capabilities of a skate.

To make a comparison between these different types of sensing systems (artificial and natural), a study must first be made of the noise fields in which these different systems are found. The dominant component of the noise field surrounding sensing systems located above the ocean's surface is the vertical component (perpendicular to the ocean's surface) and consists mainly of lightning noise (atmospherics) as well as noises of ionospheric origin. The extensive studies of atmospheric noise conducted in recent years (Refs. 16 and 17) have shown that in the range of frequencies of interest ($f \lesssim 10$ Hz), the vertical component of the electrical noise field was near 50 dB relative to 1 $\mu V/m/\sqrt{Hz}$.‡

In the ocean, sources of natural noise are much more numerous, and atmospheric noises are not as dominant in the ocean as in air. The reason for this decrease in amplitude of atmospheric noise is that in the ocean, the dominant component of the atmospheric noise field is the tangential component, E_{tan}^{sea}, parallel to the ocean's surface. This component is related to the dominant vertical component of the noise field just above the surface, E_{vert}^{air}, by the following relation (Ref. 14):

$$E_{tan}^{sea} = 3.76 \times 10^{-6} \sqrt{f}\, E_{vert}^{air} \qquad (44)$$

The findings of Section 3 concerning magnetic field detection by electroreceptive fish make it unnecessary to compare artificial and natural sensing systems with regard to the detection of magnetic dipoles. Clearly, based on the most recent data concerning measured thresholds of electroreceptive fish, artificial systems are far superior for purposes of magnetic dipole detection. Of course, one could obtain a reasonable estimate of the MDD of magnetic dipoles by artificial systems by the use of the appropriate field formulas (see sect 3 or Ref. 9).

***The electric signal source for this type of system is presumed to be a horizontal, electric dipole submerged in the ocean at a depth not lower than one or two skin depths.*

†*The use of multielement sensing arrays will undoubtedly increase the MDD of artificial systems. However, the analysis of a single-element array should give a reasonable estimate of the lower bound on the MDD of artificial systems. For an excellent review of multielement arrays, see (Ref. 15).*

‡*This value did not vary a great deal for different locations or times. It is assumed here that this noise level is fairly representative of noise levels over the sea at these frequencies. Of course, this assumption may not be valid, and more noise data over the sea at extremely low frequencies is needed.*

For f $\lesssim$ 10 Hz, Eq. (44) indicates that in the ocean, atmospheric noise is down by at least 100 dB from its levels in the air just above the ocean's surface. Actually, this figure of 100 dB loss does not include the exponential attenuation $e^{-\ell/\delta}$, where $\delta = \sqrt{2/\omega\mu\sigma}$ and ℓ is the depth of noise penetration. However, at the low frequencies we are considering, such attenuation can be neglected down to depths of approximately 100 m since $\delta \approx 70$ m at 10 Hz. Of course, it is this exponential attenuation which blocks out atmospheric noise in the ocean at frequencies greater than 100 Hz (Ref. 10).

Therefore, according to Eq. (44) and the data of Ref. 16, it is seen that in the ocean (within a skin depth of the ocean's surface) the tangential component of the atmospheric electrical noise is approximately -50 dB relative to 1 μV/m/$\sqrt{\text{Hz}}$ for f $\lesssim$ 10 Hz. This noise level seems to be of little consequence to the passive electric sensing system of skates. Of course, there are other sources of noise in the ocean. Kalmijn (Ref. 1), in an excellent review paper, has mentioned several sources of electrical noise which may influence electric-sensing systems in the ocean. Among the different types which are mentioned are noise fields due to ocean currents flowing through the earth's magnetic field (measured noise fields up to 50 μV/m); noise fields due to geomagnetic variations (measured noise fields on land up to 100 μV/m – measured noise fields in the ocean – in coastal waters and along the continental shelf – up to 10 μV/m); noise fields of electrochemical origin (no available data); and noise fields of biological origin. Indications are that due to the wide variety of such noises, noise fields in the ocean ***might*** reach levels comparable to atmospheric noise in air. However, more measurements of electric field (as well as magnetic field) noise at various places in the ocean and at different times are needed.*

Therefore, due to the scarcity of noise data in the ocean, it will be assumed that the background noise in the ocean at extremely low frequencies consists mainly of atmospheric noise at a level of -50 dB relative to 1 μV/m/$\sqrt{\text{Hz}}$. (Actually, this is probably a good assumption down to 5 Hz (see Ref. 10). From 0–5 Hz, the other sources of noise mentioned above will most likely start to contribute to ocean noise**. At this point, it should be noted that if actual noise levels in the ocean are, indeed, much greater than -50 dB, then a study of the signal processing capabilities of electrosensing fish might be needed (especially if the ocean noise levels were found to be much above 0 dB relative to 1 μV/m/$\sqrt{\text{Hz}}$) for an adequate comparison between artificial and natural sensing systems. Of course, it is quite reasonable to assume that skates and electroreceptive fish in general have developed, through evolution, a very sophisticated signal processor which is quite capable of detecting extremely low frequency signals (bioelectric fields, for instance) in the presence of a great deal of noise.†

Based on the results of this report and the assumptions stated above, it is seen that the MDD of skates at frequencies below 10 Hz is approximately 100 m (see Sections 3B and 4). (It is important to note that this value of 100 m corresponds to $I\ell = 4\pi\sigma \approx 60$ A-m. However, since we will assume a source current moment approximately 60 A-m for all systems, this value is not too important since it is only a *relative* comparison between the artificial and natural systems that is sought.) The MDD values of the two different artificial

---

**Liebermann (Ref. 10) has reported some data on the spectrum of natural geomagnetic noises in the ocean.*

***With regard to electric field noises in the 5–80-Hz range off the coast of Baja California, see the article by Soderberg (Ref. 18). Soderberg's data for depths between 30–300 m agrees (approximately) with the assumed value given above, i.e., -50 dB relative to 1 μV/m/$\sqrt{Hz}$.*

†For the detection of signals by fresh water electroreceptive fish in the presence of lightning noise, see the article by Hopkins (Ref. 19).

systems mentioned previously will now be compared with this value of 100 m for the skates. First to be considered is the artificial underwater system. As stated above, this system consists of an electric field sensing antenna connected to a bandpass filter and voltage sensor. The filter bandwidth will be assumed to be 1 Hz* and the sensitivity of the voltage sensor will be assumed to be approximately 10 nV. (This value of 10 nV sensitivity is obtainable with voltage sensors presently on the market. See Ref. 24.)

For the optimum design of this system, the noise level present in the system will be considered first. This noise consists mainly of the ocean noise which, as assumed above, is horizontal to the ocean's surface and is at a level of -50 dB relative to 1 $\mu V/m/\sqrt{Hz}$, or 3×10^{-9} $V/m/\sqrt{Hz}$. Since the filter bandwidth is assumed to be 1 Hz, it is seen that the smallest electrical field signal which can be detected is 3×10^{-9} V/m (assuming that the lowest possible filter output signal-to-noise ratio (SNR) for signal detection is 1).

Assume now that the sensor system (filter plus voltage sensor) is connected to an electric field sensing antenna (conducting plates, long wire, toroid, etc.) which is aligned parallel to the direction of the incoming electric field vector. Then, the magnitude of the open-circuit voltage which is sensed by the voltage sensor is given by $v = |\underline{\ell}_{eff} \cdot \underline{E}^{inc}|$, where $\underline{\ell}_{eff}$ is the effective length of the antenna and $\underline{E}^{inc}$ is the incoming electric field. It is noted that the effective length of an antenna is not always the same as the antenna's actual physical length. (See, for example, Chap. 4 of Ref. 25.) In general, an antenna's effective length depends on the frequency of operation, the external medium, etc.** By choosing a sensing antenna with an appropriate effective length, one can detect an incident signal field of 3×10^{-9} V/m and yet have the voltage signal at the input of the voltage sensor above its 10-nV sensitivity. For instance, by connecting the sensor to an antenna with an effective length of approximately 3 m ($\approx 10^{-8}$ V/3×10^{-9} V/m), it is possible to detect an incident signal field of 3×10^{-9} V/m. On the basis of Figs. 4, 5, and 6, this would correspond to an MDD of approximately 0.5 km at 1 Hz, and an MDD of approximately 0.4 km at 10 Hz. For detection of direct-path signals with $I\ell \approx 60$ A-m, see Fig. 13. As seen in Fig. 12, 3×10^{-9} V/m corresponds to an MDD of approximately 1 km [for detection by the up-over-and-down path with $I\ell \approx 60$ A-m and with the source electric dipole assumed to be horizontal (Fig. 14)]. Therefore, from the above considerations, the MDD of the artificial system described above will be set at approximately 0.5 km for direct-path detection over the 1- to 10-Hz range.† When the electric dipole is approximately horizontal and the combined depth of the dipole source and electric sensor is less than a skin depth, the MDD of this underwater system is 1 km for the indirect path detection over the 1- to 10-Hz range. Of

---

A fixed-bandpass filter with bandwidth 1 Hz is considered in this report for the sake of simplicity in the following comparisons. Of course, other types of filters might be more desirable than the fixed-bandpass type. For instance, adaptive-type filters may be desired for their ability to track frequency drifts in the input signal. See, for example, Widrow (Ref. 20), Widrow, et al., (Ref. 21), Zeidler and Chabries (Ref. 22), and Griffiths (Ref. 23).

***Swain (Ref. 26) has shown that the effective length of a tuned toroid antenna in a conducting medium can be made very long as compared to the physical dimensions of the toroid. By inserting a long, highly conducting core in the center of the toroid, its effective length can be made even longer (Ref. 27).*

†By submerging the sensing antenna at very great depths (greater than 3 skin depths), ocean noise will be reduced at the voltage sensor input (at least in the 5- to 10-Hz range) due to exponential attenuation as noted previously. Therefore, the MDD of the underwater system will be raised somewhat over the 0.5-km value given above just by lowering the system deeper in the ocean. However, the MDD value will not be raised by very much because of the exponential attenuation of the signals. Therefore, the 0.5-km value for the MDD for direct-path detection is a reasonable estimate.

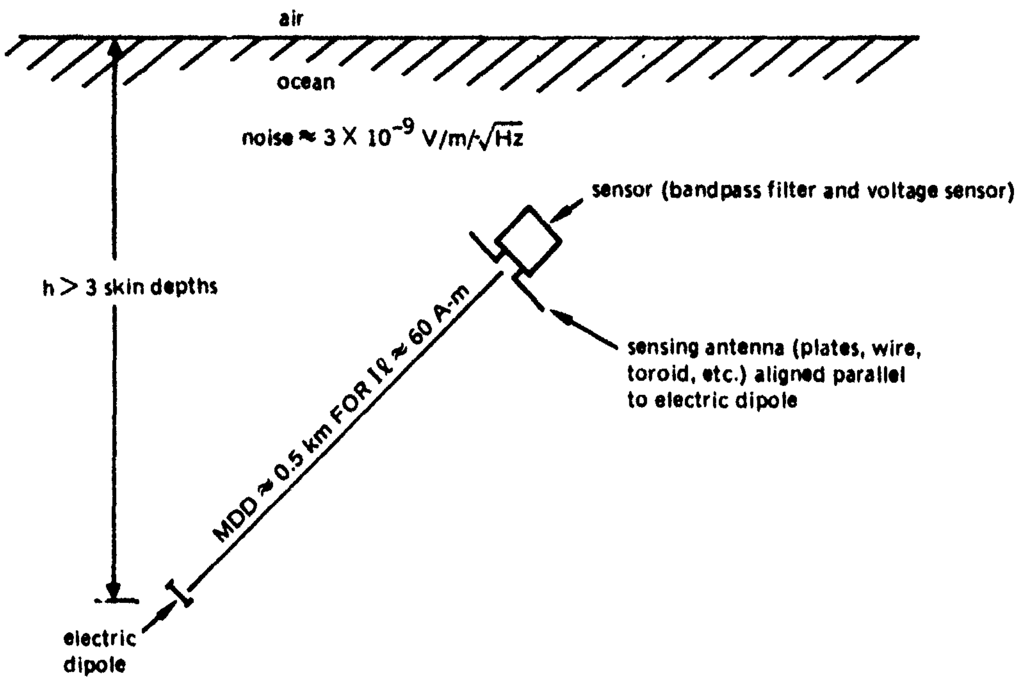

Figure 13. Direct-path detection alignment for underwater system for $f \approx 1$–10 Hz (not drawn to scale).

course, these MDD values are probably somewhat optimistic since the ocean noise fields are most likely more intense than the assumed level (3×10^{-9} V/m/$\sqrt{\mathrm{Hz}}$), at least in the 0- to 5-Hz frequency range.

The second type of artificial sensing system (for detecting horizontal electric dipoles) to be considered consists of a single sensing antenna placed above the ocean's surface. Once again, it is assumed that the antenna is connected to the sensing system described above. In this case, the vertical component of the electric noise field (just above the ocean's surface) is 50 dB above 1 μV/m/$\sqrt{\mathrm{Hz}}$ as noted above, or, equivalently, 3×10^{-4} V/m/$\sqrt{\mathrm{Hz}}$, and the horizontal component of the electric noise field (just above the ocean's surface) is 3×10^{-9} V/m/$\sqrt{\mathrm{Hz}}$. Using a magnetic field sensing antenna as well as an electric field sensing antenna in this system is also a possibility. In this regard it is noted that the horizontal component of the magnetic noise field just above the ocean's surface in the extremely low-frequency range ($f \lesssim 10$ Hz) is approximately 10^{-6} A/m/$\sqrt{\mathrm{Hz}}$ (Ref. 16). Since the filter bandwidth considered in this report is 1 Hz, it is noted that the smallest vertical electrical field signal which can be detected (for output SNR of 1) is 3×10^{-4} V/m, which is about 300 times greater than the skate threshold. The smallest detectable horizontal electric field signal is 3×10^{-9} V/m and the smallest detectable horizontal magnetic field signal is 10^{-6} A/m.

A vertical electric field, horizontal electric field, or horizontal magnetic field at these magnitudes (3×10^{-4} V/m, 3×10^{-9} V/m and 10^{-6} A/m, respectively) can be

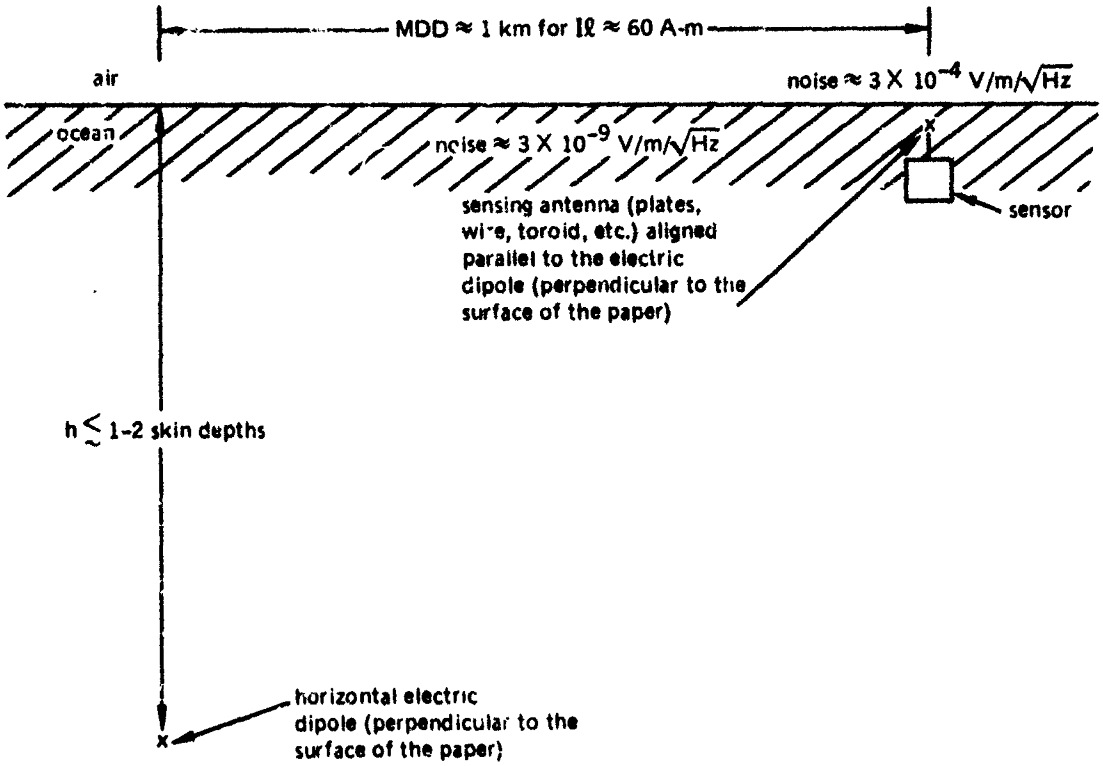

Figure 14. Indirect-path detection alignment for underwater system for f = 1–10 Hz (not drawn to scale).

detected by the sensor system connected to an electric field sensing antenna or a magnetic field sensing antenna. A vertical electric field sensing antenna with an effective length of less than 1 m can be used to detect the vertical component of electric fields on the order of 3×10^{-4} V/m. Referring to Fig. 12, we see that the MDD of this system with a vertical electric field sensing antenna (for source depth not greater than a skin depth) is less than 0.1 km for $I\ell \approx 60$ A-m and for f = 1–10 Hz. By analogy with the underwater system, the MDD of this system with a horizontal electric field sensing antenna placed just above the ocean's surface is approximately 1 km. Use of a magnetic field sensing antenna (a loop will be considered) will increase the MDD of this system somewhat. From Ref. 28, it can be seen that the magnitude of the voltage sensed by a core-loaded loop is given by $V = \mu_e \omega H^{inc} \cdot AN$, where H^{inc} is the magnitude of the incident magnetic field; A is the area of the loop; N is the number of turns of wire in the loop; and $\mu_e = \mu \cdot \mu_r/(1 + D(\mu_r - 1))$, where μ_r is the* relative permeability of the core and D is a dimensionless parameter related to the shape of the core (D = 0 for long thin cores; D = 1/3 for spherical cores; and D = 1 for cores in the shape of thin disks). From this formula it can be seen that a loop with an area of 1 m^2 and 10 turns loaded with a long thin core ($D \sim 0$) of high permeability ($\mu_r \sim 100$) could sense a voltage of approximately 10 nV for an incident horizontal magnetic field of magnitude 10^{-6} A/m at 1–10 Hz.

---

*$\mu = 4\pi \times 10^{-7}$ *henries/m.*

The dominant horizontal component of the magnetic field just above the ocean's surface which is generated by a horizontal electric dipole at a depth h below the ocean's surface is given by (Ref. 9, p. 209):

$$H_{2r} = \frac{I\ell \sin\phi}{\pi \gamma r^3} e^{-\gamma h} \tag{45}$$

where all symbols are as defined in section 4. Therefore, assuming correct hookup of the properly aligned, core-loaded loop described above to the voltage sensor and filter, the MDD of this system is approximately 2.5 km for both 1 Hz and 10 Hz and for $I\ell \approx 60$ A-m (assuming, of course, that h is within one – at most two – skin depths of the ocean's surface). Thus by using a magnetic field sensing antenna (core-loaded loop) in this system, the MDD of this system can be increased to approximately 2.5 km (for detection by the indirect path) at 1 Hz and 10 Hz and $I\ell \approx 60$ A-m. (See Fig. 15 for the proper alignment of this system.)

It is now possible to compare the different types of artificial and natural sensing systems. It is seen that for detecting extremely low-frequency, narrowband signals which are generated by horizontal electric dipoles within a skin depth (or two) of the ocean's surface, the best type of sensing system is either the underwater artificial system (Fig. 14) or the artificial system which is placed just above the ocean's surface (Fig. 15). The MDD for

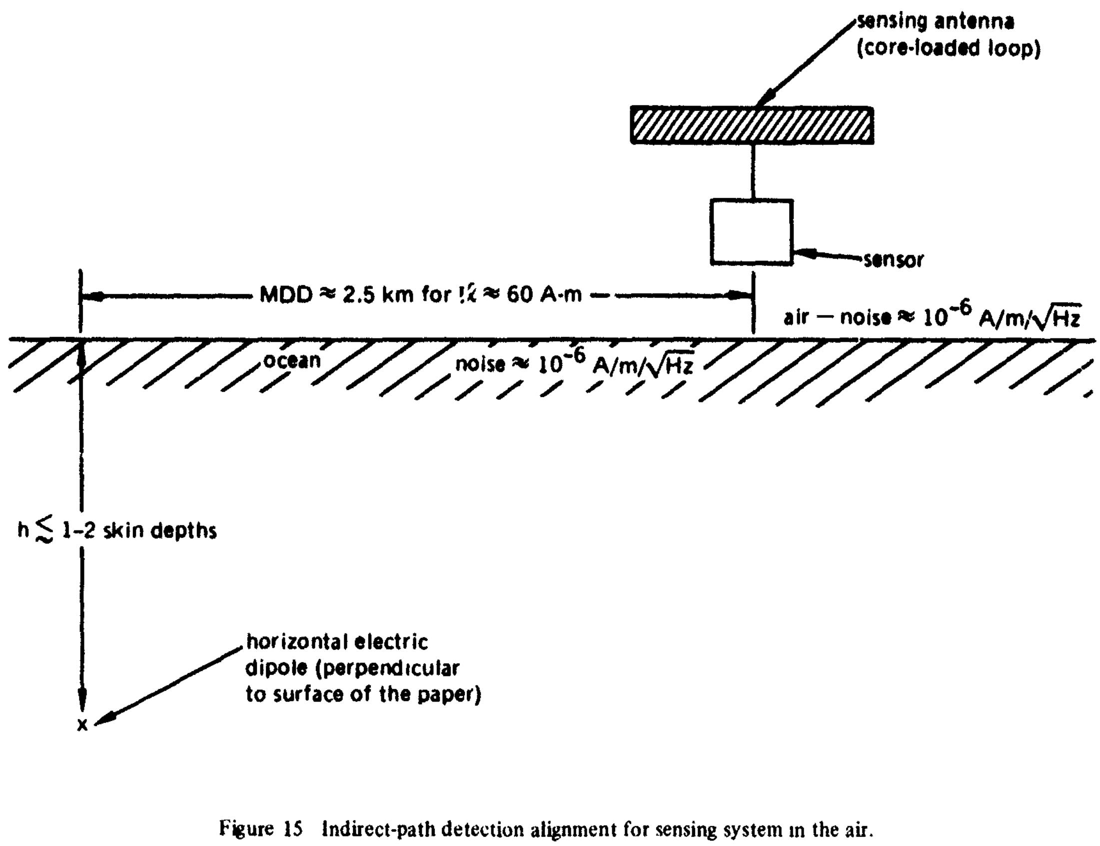

Figure 15 Indirect-path detection alignment for sensing system in the air.

either system is approximately 2.5 km* (for $I\ell \approx 60$ A-m and f = 1–10 Hz) which is approximately 25 times better than the MDD of a skate (*Raja clavata*) ($\approx$ 100 m also at $I\ell \approx 60$ A-m and f = 1–10 Hz). For detecting signals generated by sources deeply submerged in the ocean (greater than 2–3 skin depths), the best type of sensing system is the artificial underwater sensing system (Fig. 13) with an MDD of approximately 0.5 km (for $I\ell \approx 60$ A-m and f = 1–10 Hz) as compared to 100 m (also at $I\ell \approx 60$ A-m and f = 1–10 Hz) for the skate. Therefore, man-made systems *seem* to be superior for the long-range detection of narrowband, extremely low-frequency signals.

Of course, it should be pointed out that in this section, no restrictions were placed on the effective length of the antennas used in the man-made system (viz., we have chosen antennas with effective lengths of 3 meters), whereas the effective length of the skate's antenna is restricted to its maximum ampullary canal length, which is approximately 20 cm (Ref. 29). Therefore, it could be argued that the above comparisons are not fair and that to make a better comparison, the effective lengths of the man-made antennas should be restricted to approximately 20 cm. However, what was desired in this section was a comparison between the optimum, single-element man-made system and the optimum biological system (i.e., the skate). Therefore, no restrictions were placed on the effective length of the antenna used in the man-made system. In fact, the only factor which limits the effective length is noise (atmospheric noise, etc.). The results of this section show that man-made systems can sense down to the level of electric field noise in the ocean, while the optimum biological system is apparently not this sensitive (see page 24). Even if a comparison between the sensitivity of the optimum biological system and a man-made system of comparable effective length (20 cm) had been desired, the man-made system would still have fared better than the skate (viz., the sensitivity of the man-made system with a 20-cm antenna is approximately 10 nV/0.2m = 5×10^{-8} V/m, as compared to 10^{-6} V/m sensitivity for the skate).

The above conclusions concerning the apparent superiority of man-made systems over the skate are not too surprising when one considers that the passive electrosensing of electroreceptive fish in the ocean (especially the bottom feeders) is designed mainly for the detection of very short-range bioelectric fields which emanate from prey that may be buried in the sand. It is not important to the electroreceptive fish to detect an electrical signal many miles away, only at a very short range. Of course, more data are needed on the electric field thresholds of electroreceptive fish of different species, sizes, shapes, etc. New data might indicate that electrosensing fish could detect electric objects at much greater distances than indicated in this report.

Actually, according to the above analysis, the MDD of the underwater system consisting of an electric field sensing antenna placed just below the ocean's surface is approximately one-half the MDD of the sensing system placed just above the ocean's surface which employs a magnetic field sensing antenna. However, by using a magnetic field sensing antenna for the underwater sensing system, the MDD of this system will be exactly the same as the MDD of the sensing system placed above the ocean's surface (based on our assumptions concerning noise)

6. CONCLUSIONS

SUMMARY

In this report the possibility of the detection of dipole fields by electrosensing fish has been considered. In particular, a skate (*Raja clavata*) which is sensitive to threshold electric fields of 1 μV/m has been examined. This value represents the highest electrical sensitivity known in aquatic animals. The results, presented in Sections 3 and 4, indicate that skates detect electric dipole fields (either by the direct path of propagation through the water (Section 3) or by the up-over-and-down path of propagation (Section 4) at relatively short distances (approximately 100 m at f = 0, 1, or 10 Hz and for source current moments on the order of 60 A-m). As pointed out in Section 3, electrosensing fish can also detect the electric field component of a magnetic dipole source as well as the magnetic field components of both magnetic and electric dipole sources (by moving relative to the magnetic fields), but detection of these components is limited to very short ranges (approximately 7 m for either magnetic dipole moments of 4π A-m^2 or electric dipole moments of approximately 60 A-m at f = 0, 1, and 10 Hz).

In Section 5, a comparison is made between the electric dipole sensing capabilities of skates and artificial systems. In particular, two different types of artificial sensing systems were considered. The first was a system for underwater use and the second was a sensing system to be used over the ocean's surface for detecting electric dipole sources submerged at depths not greater than one or two skin depths. It was found that for purposes of detecting electric dipoles submerged deep in the ocean (at depths greater than two or three skin depths), the best type of sensing system is the artificial underwater sensing system. For electric dipoles submerged at depths which are less than one or two skin depths, the best type of sensing system is the artificial system that is placed either just above the ocean's surface or just below the ocean's surface. Of course, the conclusions reached above are subject to certain assumptions, which are explicitly stated in Section 5. It is hoped that these considerations in Section 5 will provide a reasonable estimate of the lower bound on the maximum detection distance of electric dipoles by artificial systems.

SUGGESTIONS FOR FURTHER WORK

It is rather clear that much more work needs to be done in the area of electromagnetic sensing by electroreceptive fish (or perhaps "magnetic" fish). Some of the areas for future work, as suggested by this report, include the study of magnetic-sensing capabilities of different types of aquatic animals. Measurements of the effects of magnetic fields on biological systems in general have been initiated (see, for instance, Ref. 30), however, measurements of magnetic thresholds of aquatic animals are not quite as numerous. As pointed out in Section 3, hypothetical "magnetic" fish sensitive to magnetic fields of 1 μA/m (0.001

gamma)*, could sense electric dipole fields further away than electric sensing fish sensitive to 1 μV/m. However, to determine if fish are sensitive to variations as small as fractions of gammas in a constant background magnetic field of 0.5 gauss would require incredible experimental accuracy. First, all background noises would have to be cancelled, and then a constant background field of 0.5 gauss in addition to a well controlled, very small-amplitude magnetic field (on the order of gammas or less) would be applied to the fish. Unfortunately, the big problem arises when one tries to shield out small-amplitude, magnetic-noise fluctuations. The cheaper magnetic shields effectively block out magnetic noise variations only down to tens of gammas in a relatively small volume. As an example, Helmholtz coils can reduce the magnetic field over a control volume of about 100 cc to less than ±50 gammas. The cost of reducing magnetic noise fields to the order of gammas or less (over relatively large volumes $\gtrsim 1\ m^3$) can become quite prohibitive. Therefore, shielding costs are so high that low-amplitude magnetic-threshold measurements on aquatic animals are quite expensive.

Another area for future work is the continued measurements of the electric field thresholds of electrosensing fish. Specifically, measurements of electric field sensitivities of sharks and skates of different lengths should be undertaken to determine whether longer electroreceptive fish are, as suggested by Kalmijn (Ref. 1), indeed more sensitive. Such measurements could be extremely useful as a further check on our models of passive electroreception by sharks and skates. Of course, as mentioned in Section 5, more data on the electric field thresholds of electric fish of different species are also needed. Finally, the need for further measurements of electromagnetic noise occurring in the ocean is mentioned. Indications are that at certain points in the ocean, electromagnetic noise might be quite larger than the lowest thresholds of skates, 1 μV/m (see Section 5). Such measurements, therefore, could possibly aid in our understanding of the degree of signal processing which occurs in certain electric fish. This knowledge might be of use in the design of artificial signal processors.

This report has treated, mainly, passive electrosensing fish. Of course, electrogenic fish also exist (Ref. 2), i.e., fish capable of creating their own electric field for the purposes of detecting objects and communicating with other fish. A quantitative look at the electric fields produced by these fish as well as the distortions in these fields which are caused by objects placed in the fields might be of use in the design of artificial active electromagnetic sensing systems for use either in fresh water or in the ocean.

Quite properly, these hypothetical fish would be sensitive to magnetic field variations of 0.001 gamma within the earth's background magnetic field ($\approx$ 0.5 gauss)

REFERENCES

1. A. J. Kalmijn, "The Detection of Electric Fields from Inanimate and Animate Sources Other than Electric Organs", chap. 5 in *Handbook of Sensory Physiology III*, A. Fessard, ed. New York: Springer-Verlag, 1974.

2. H. Scheich and T. H. Bullock, "The Detection of Electric Fields from Electric Organs", chap. 6 in *Handbook of Sensory Physiology III*, A. Fessard, ed. New York: Springer-Verlag, 1974.

3. T. H. Bullock, "Seeing the world through a new sense: electroreception in fish", *American Scientist*, vol. 61, May 1973, pp. 316-325.

4. A. J. Kalmijn, "The electric sense of sharks and rays", *J. Exp. Biol.* (1971), *55*, pp. 371-383.

5. M. B. Kraichman, *Handbook of Electromagnetic Propagation in Conducting Media,* NAVMAT P-2302, Headquarters Naval Material Command, 1970.

6. J. R. Wait, "Electromagnetic Fields of Sources in Lossy Media," in *Antenna Theory,* Part II, R. E. Collin and F. J. Zucker, ed., PP. 438-514, McGraw-Hill, New York, 1969.

7. C. H. Papas, *Theory of Electromagnetic Wave Propagation,* McGraw-Hill, New York, 1965.

8. J. D. Jackson, *Classical Electrodynamics,* John Wiley & Sons, Inc., New York, 1962.

9. A. Baños, *Dipole Radiation in the Presence of Conducting Half-Space*, Pergamon Press, Oxford, 1966.

10. L. N. Liebermann, "Other electromagnetic radiation", in *The Sea*, M. N. Hill, ed., vol. 1, pp. 469–475, Wiley, New York, 1962.

11. H. Mott and A. W. Biggs, "Very-Low-Frequency propagation below the bottom of the sea", *IEEE Transactions*, vol. AP-11, No. 3, May 1963, pp. 323–329.

12. R. K. Moore, "Radio Communication in the Sea," *IEEE Spectrum,* Nov. 1967, pp. 42–51.

13. A. Sommerfeld, "Uber die Ausbreitung der Wellen in eber drahtlosen Telegraphie," *Ann. Physik* 28, 665–737, 1909.

14. W. L. Anderson, "The Fields of Electric Dipoles in Sea Water – the Earth-Air-Ionosphere Problem," Tech. Rept., EE-88, Engineer. Expt. Station, Univ. of New Mexico; Albuquerque, New Mexico, May, 1963.

15. A. A. Ksienski, "Signal-Processing Antennas," in *Antenna Theory, Part II,* R. E. Collin and F. J. Zucker, eds., pp. 580–654, McGraw-Hill, New York, 1969.

16. E. L. Maxwell and D. L. Stone, "Natural noise fields from 1 cps to 100 kc", *IEEE Transactions*, vol. AP-11, No. 3, May 1963, pp. 339-343.

17. "World Distribution and Characteristics of Atmospheric Radio Noise", CCIR Rept. 322, Documents of the Xth Plenary Assembly, Geneva, 1963. Published by International Telecommunications Union, Geneva, 1964.

18. E. F. Soderberg, "ELF noise in the sea at depths from 30 to 300 meters", *J. of Geophysical Res., 74,* 2376–2387, (1969).

19. C. D. Hopkins, "Lightning as background noise for communication among electric fish", *Nature* (London), vol. 242, pp. 268–270 (1973).

20. B. Widrow, "Adaptive Filters", In: *Aspects of Network and System Theory,* R. E. Kalman and N. Deelaris, eds., Holt, Rhinehart & Winston, Inc., New York, 1971.

21. B. Widrow, J. R. Glover, J. McCool, et al., "Adaptive Noise Cancelling: Principles and Applications," *IEEE Proc.* Vol. 63, No. 12, Dec. 1975, pp. 1692–1716.

22. Naval Undersea Center, NUC TN 1476, An Analysis of the LMS Adaptive Filter used as a Spectral Line Enhancer, by J. R. Zeidler, D. M. Chabries, Feb. 1975.

23. L. J. Griffiths, "Rapid Measurement of Digital Instantaneous Frequency", *IEEE Transactions,* Vol. ASSP-23, No. 2, April 1975, pp. 207–222.

24. Teledyne Crystalonic Data Sheet for C413N Silicon Epitaxial Junction N-Channel Field Effect Transistor. Available from: Teledyne Crystalonics; 2082 S.E. Bristol St., Suite #4, Newport Beach, CA 92707.

25. *Antenna Theory, Part I,* R. E. Collin and F. J. Zucker, eds., McGraw-Hill, New York, 1969.

26. G. R. Swain, "A Small Magnetic Toroid Antenna Embedded in a Highly Conducting Half-Space", *J. Res. NBS,* Vol. 69D, No. 4, (1965), pp. 659–665.

27. R. H. Williams, R. D. Kelly, and W. T. Cowan, "Small Prolate Spheroidal Antenna in a Dissipative Medium," *J. Res. NBS,* Vol. 69D, No. 7, (1965), pp. 1005–1010.

28. W. L. Weeks, *Antenna Engineering,* McGraw-Hill, New York, 1968.

29. Private communication with E. I. Knudsen, Scripps Institution of Oceanography.

30. *Biological Effects of Magnetic Fields,* Vol. II, M. F. Barnothy, ed., Plenum Press, New York, 1969.